Original scientific paper
Accepted 29. 12. 2014.

GUNTER WEISS
SYBILLE MICK

Non-standard Visualizations of Fibonacci Numbers and the Golden Mean

Dedicated to Prof. Dr. Otto Röschel on the occasion of his 60^{th} birthday.

Non-standard Visualizations of Fibonacci Numbers and the Golden Mean

ABSTRACT

Fibonacci numbers and the Golden Mean are numbers and thus 0-dimensional objects. Usually, they are visualized in the Euclidean plane using squares and rectangles in a spiral arrangement. The Golden Mean, as a ratio, is an affine geometric concept and therefore Euclidean visualizations are not mandatory. There are attempts to visualize the Fibonacci number sequence and Golden Spirals in higher dimensions [11], in Minkowski planes [12], [4] and in hyperbolic planes (again [4]). The latter has to replace the not existing squares by sequences of touching circles. This article aims at visualizations in all Cayley-Klein planes and makes use of three different visualization ideas: nested sets of squares, sets of touching circles and sets of triangles that are related to Euclidean right angled triangles.

Key words: Cayley-Klein geometries, Fibonacci numbers, Golden Mean

MSC 2010: 51M04, 51M10, 51F20, 11B39

Nestandardne vizualizacije Fibonaccijevih brojeva i zlatni rez

SAŽETAK

Fibonaccijevi brojevi i zlatni rez su brojevi, stoga su to 0-dimenzionalni objekti. Najčešće se vizulaiziraju u euklidskoj ravnini, pomoću kvadrata i pravokutnika u spiralnom poretku. Zlatni rez, kao omjer, je pojam afine geometrije pa euklidske vizualizacije nisu nužne. Postoje pokušaji vizualizacije Fibonaccijevog niza i zlatne spirale u višim dimenzijama [11], u ravninama Minkowskog [12], [4], i u hiperboličkim ravninama, također [4], gdje se nepostojeći kvadrati zamjenjuju kružnicama koje se dodiruju. Cilj ovog rada je vizualizacija u svim Cayley-Kleinovim ravninama uz korištenje triju različitih ideja: grupiranih skupova kvadrata, skupova kružnica koje se dodiruju i skupova trokuta koji su analogni euklidskim pravokutnim trokutima.

Ključne riječi: Cayley-Kleinove geometrije, Fibonaccijevi brojevi, zlatni rez

1 Euclidean Visualizations

In this paper we continue a study of visualizing the classical sequence of Fibonacci numbers and Golden Spirals [4] and aim at visualizations in general Cayley-Klein planes.

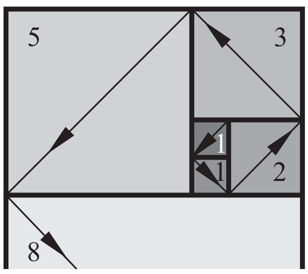

Figure 1: *Set of Fibonacci squares*

In the Euclidean plane there are mainly three cases:

(α) The standard visualization by nested sets of Golden Rectangles and gnomon squares, see Figures 1, 2 and e.g. [1], [4], [14]. Inscribing quarter circles into the gnomon squares results in discrete spirals of C^1-continuity.

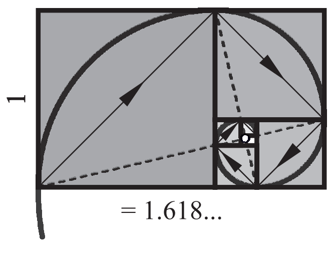

Figure 2: *Nested set of Golden rectangles and quater circle biarc spiral*

(β) In [4] the authors propose to use a chain of circles where each circle touches the former two circles, see Figures 3, 4. This type of visualization even allows generally normed planes (Minkowski planes) and also a hyperbolic plane as places of action, i.e. planes without a (proper) concept of squares.

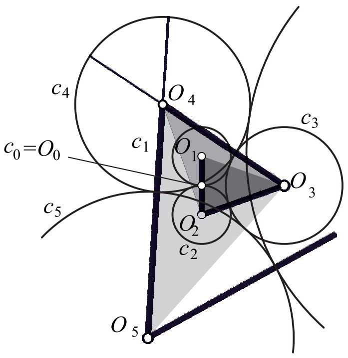

Figure 3: *Set of touching Fibonacci circles and Fibonacci spiral polygon of circle centres*

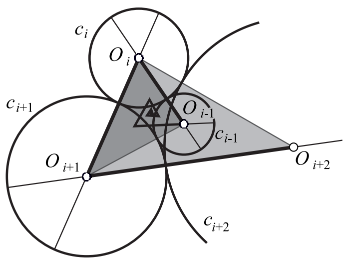

Figure 4: *Set of "Golden Circles" and spiral polygon of circle centres*

From the construction of touching circles in Figure 3 follows that we get a limit triangle of circle centres with side ratio

$$a:b:c = F_{i+1}:(F_{i-1}+F_{i+1}):F_{i+2} = 1:(1+\frac{1}{\phi^2}):\phi$$
$$= (1+\phi):(2+\phi):(1+2\phi). \quad (1)$$

Figure 4 contains a nested set of such triangles with side ratio (1).

(γ) In this paper we propose an additional way of visualizing Fibonacci numbers and Golden spirals using sets of Pythagoras triplets and right angled triangles akin to the classical root spiral. Similar to Fibonaccis rule Pythagoras formula adds two numbers and gives a new one. This in mind, one can generate the set of natural numbers as well as the Fibonacci sequence via iterative processes applied to the classical formula of Pythagoras, see Figure 5.

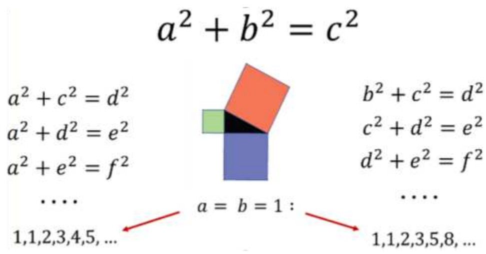

Figure 5: *Natural numbers and Fibonacci numbers derived from Pythagoras' formula*

While the left column leads to the so-called root-spiral and triangles with cathetes $\sqrt{n}, 1$ and the hypotenuse $\sqrt{n+1}$, see Figure 6, the right column leads to cathetes $\sqrt{F_{i-1}}$, $\sqrt{F_i}$ and the hypotenuse $\sqrt{F_{i+1}}$, see Figure 7. Again, we get a 'limit' triangle with side ratio

$$a:b:c = \sqrt{F_{i-1}}:\sqrt{F_i}:\sqrt{F_{i+1}} \quad (2)$$

Such a triangle might as well be called Golden (right-angled) Triangle. Figure 8 shows the spiral polygon derived from such Golden Triangles.

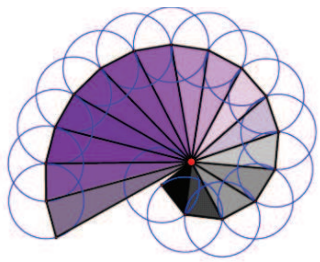

Figure 6: *The classical "root spiral"*

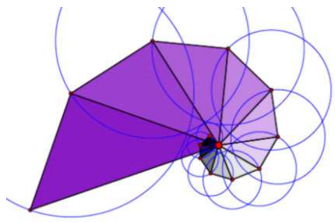

Figure 7: *Fibonacci number root spiral*

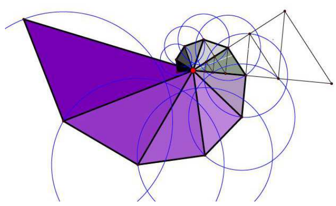

Figure 8: *Golden Root Spiral Polygon*

While in the Euclidean plane triangles with side ratio (2) are right angled by themselves, this is not the case in the hyperbolic plane. But as long the triangle in-equation for the side ratio (2) remains valid this third type of visualizations is also possible in a wide range of settings as it is shown in the following chapters. It should be mentioned that the ratio (2) is supposed to be connected with some of the ancient Egyptian pyramids, c.f. the concepts "Kepler triangle" and "Golden Pyramid", see [14].

2 The Golden Mean and the Fibonacci-sequence

There is such a huge number of publications dealing with the Golden Mean and Fibonacci numbers and the topic has become common knowledge among mathematicians that one can refrain from citing more than a few basic books on that theme, e.g. [1], [9] and the Wikipedia article [14] which contains a long list of references.

Fibonacci numbers and the Golden Mean value ϕ are numbers, thereby ϕ is a root of $x^2-x-1=0$ and the result of the "most irrational continued fraction" $\phi = 1+\frac{1}{1+\frac{1}{\cdots}}$. Being *numbers*, these objects are 0-dimensional. As a "ratio of 3 collinear points" ϕ has a 1-dimensional visualization and it is an affine geometric concept independent from any Euclidean structure. Obviously, 2-dimensional visualizations in the Euclidean plane using squares or circles cannot be mandatory! Visualizations in other settings are at least possible and might even enjoy some aesthetic value. Such non-standard visualizations also give some deeper insight into the interplay of visualization assumptions and the structure of the places of action. This might justify the following considerations.

3 Other places of action

At first we collect those visualizations in places of actions already treated in references and show some figures:

3.1 Higher dimensional Euclidean visualizations

See [11] and Figure 9.

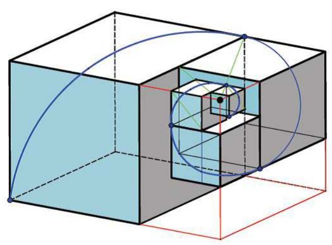

Figure 9: *Nested set of Golden Prisms with cubes as gnomon figures and a Golden helix biarc spiral*

3.2 Visualizations in (affine) normed planes (so-called Minkowski planes)

See [1], [12] and Figures 10, 11.

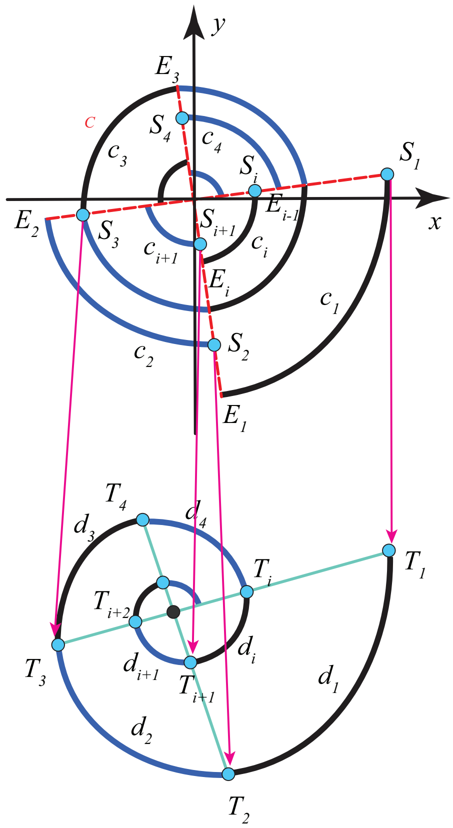

Figure 10: *Minkowski geometric analogue to Figure 2. (Applying translations τ_i to the partial arcs c_i of concentric Minkowski circles under the end-point is start-point condition results in a Minkowski circular bi-arc spiral)*

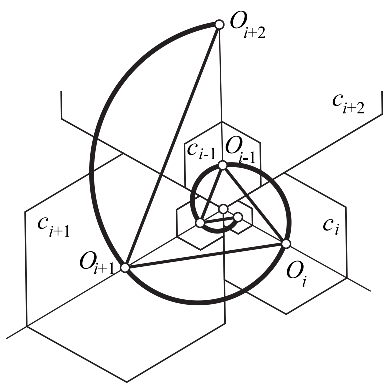

Figure 11: *Minkowski geometric analogue to Figure 4. (Sequence of touching Golden Minkowski-circles and Golden Triangles in a Minkowski plane with hexagons as circles.*

3.3 Visualizations in a hyperbolic plane

See [4] and Figure 12.

As there are no similarities and no squares in a hyperbolic plane one cannot use the visualization method (α). In [4] the authors propose method (β) and handle the different radii of the Golden circles via a hyperbolic scaled line. For visualizing the circle chain they use the F. Klein model of a hyperbolic plane and base the construction on an arbitrarily given scale on a hyperbolic line, see Figure 12.

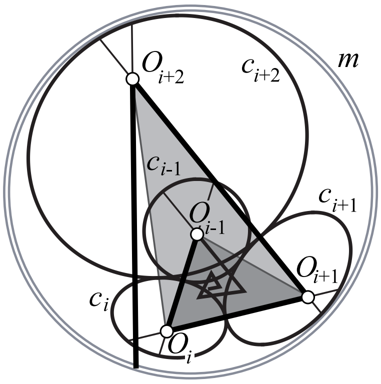

Figure 12: *A sequence of tangent Golden circles and Golden triangles in the hyperbolic plane.*

The hyperbolic case encourages us to look for visualizations also in other Cayley-Klein planes. Of course, one faces the problem of finite length of lines in e.g. the elliptic plane, while a line in affine planes and the hyperbolic plane has infinite length. It turns out that also some affine Cayley-Klein planes need greater modifications of the three visualisation schemes, as shown in the next chapters. For an overview of all Cayley-Klein planes see e.g. [3].

4 Visualisations in Cayley-Klein planes

4.1 Affine cases

4.1.1 The Euclidean case

See Chapter 1.

4.1.2 The pseudo-Euclidean case (*pe*-case)

Here, the visualization method (α) by squares does work. The constructions are based on affine parallelograms, which, by a suitably chosen affine coordinate frame can be called affine squares, affine Golden rectangles, see [4] and Figure 13.

Note that, from the pseudo-Euclidean point of view, one side of Golden Rectangles is space-like, while the other is time-like (with a negative length). Therefore one needs to modify the side ratio concept of *pe*-Golden Rectangles by using absolute values as

$$|a| : |b| = 1 : \phi. \tag{3}$$

Furthermore, the biarc spiral curve in Figure 13 consists of general conic section arcs and not of *pe*-quarter circles.

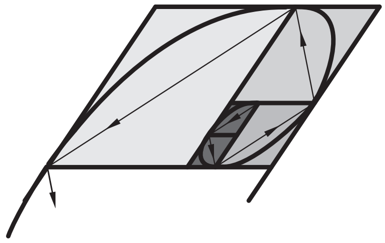

Figure 13: *"Affine Golden biarc spiral", "affine Golden Rectangles" and "squares" in an affine plane, which is endowed with a suitable affine coordinate frame.*

Method (β) does not work: It is not possible to construct a real space-like *pe*-circle (i.e. a Euclidean equilateral hyperbola with predifined directions of asymptotes), which touches two mutually touching space-like *pe*-circles. Their centres would have to form triangles with side length ratio (2). For $a < b < c$ we would have $a + b < c$, expressing that in the *pe*-plane the triangle inequality would not held.

This is why method (γ) is problematic, too. It would have to be modified according to the norm-function of the *pe*−plane by absolute values similar to (3). But as there exist the (continuous) group of *pe*-rotations, the group of translations and the group of dilatations, one can at least construct *pe*−spirals as orbits of a one-parameter group of *pe*−similarities. Generating such a discrete spiral polygon with the *pe*-similarity factor ϕ (or $\sqrt{\phi}$) then leads to a visualization of a Golden *pe*-root spiral, see Figure 14.

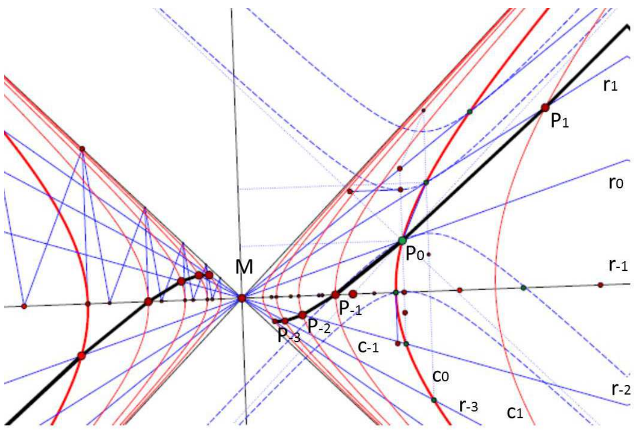

Figure 14: *Golden pseudo-Euclidean spiral polygon*

4.1.3 The isotropic case (*i*-case)

In the projective extension of an isotropic plane the ideal line u and ideal point U act as absolute figure. Choosing an affine coordinate frame $(O;E,F)$ with O,F,U collinear and E,F as unit points of the axes $x = OE, y = OU$ allows to measure the *i*-distance of two points $P(x_P,y_P)$ and $Q(x_Q,y_Q)$ as $d(P,Q) := |x_Q - x_P|$. If P,Q are collinear with U, one uses $|y_Q - y_P|$ as a substitute for their vanishing *i*-distance and calls it "spacing (Sperrung)". Obviously it is possible to construct a nested set of "Golden Rectangles" in a seemingly spiral arrangement, see Figure 15, but this affine spiral arrangement does not suit to an isotropic spiral (c.f. [7]). This way, visualization method (α) works well.

β The set of points with fixed distance to a given point is a pair of y-parallel lines, so-called isotropic lines. This circle concept is not useful for our purpose. Let us consider the following circle concept: An *i*-circle is a conic section touching the absolute line u in the absolute point U. In our model of the *i*-plane *i*-circles are parabolas with y-parallel diameters. The Euclidean parameter is a proper replacement of the concept "radius", because two *i*-circles are either similar or one is the translated of the other. It is not possible to construct an *i*-circle that touches two mutually touching *i*-circles in proper points. At least one of the tangent points must be the ideal point U. Therefore visualization method (β)is not viable.

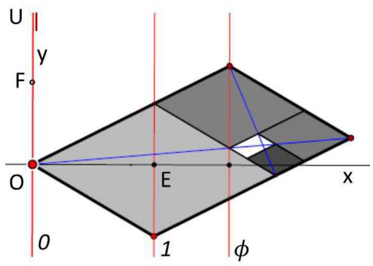

Figure 15: *Nested set of Golden Rectangles and squares in an isotropic plane.*

(γ) Similar to the *pe*-case one can generate an *i*-spiral polygon (see [7]) and can use it for the construction of a Golden *i*-root spiral, see Figure 16. For such a spiral polygon even C^1-smooth *i*-circular bi-arc spirals are possible, see Figure 17.

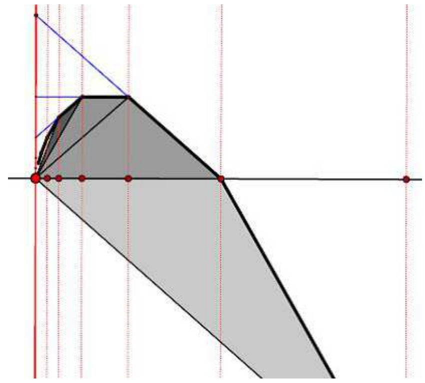

Figure 16: *Golden isotropic spiral polygon*

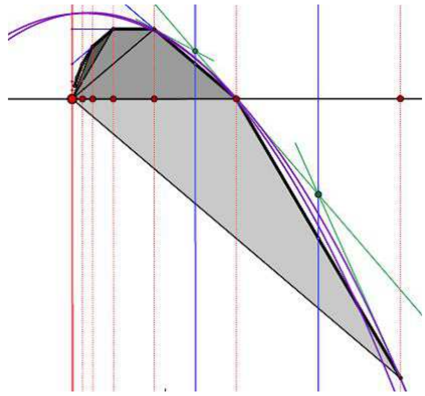

Figure 17: *i-circular biarc spiral to an i-spiral polygon*

4.1.4 The dual *pe*-plane

The dual *pe*-plane is also called quasi-hyperbolic plane (*qh*-plane). Its absolute is a pair of real lines e, f, whereby one (say $f =: u$) can act as "line at infinity" u of a projective embedding of the affine plane. Therefore, we can discuss this case in this sub-chapter. In this model of a *qh*-plane the absolute involution with the fixed lines e, f simply becomes the (Euclidean) reflection at the proper line e. Strictly speaking, the *qh*-plane is just one half-plane with respect to e, but as we did in the *pe*-plane case we also consider the projective embedding of the *qh*-structure. Applying a suitable regular polarity Ω to the pseudo-Euclidean plane one receives this model of the projectively embedded *qh*-plane, where the two half-planes represent the space-like world and the time-like world. The fixed line e represents one set of light-like lines. It is easy to translate concepts concerning ratios (of collinear points) and angles (of lines) to *qh*-ratios of lines and *qh*-angles of points. Parallel lines occur as points on a line parallel to e and orthogonal lines map to points on lines symmetric to e, such that rectangles $(ABCD)$ occur as trapecia $(abcd)$ with two sides parallel and symmetric to e. In particular, squares map to parallelograms.

For the *pe*-plane visualization method (α) can be based on Figure 13, if we modify the side ratios of the Golden Parallelograms according to (3). So we receive a visualization (α) in the *qh*-plane by dualizing Figure 13, see Figure 18.

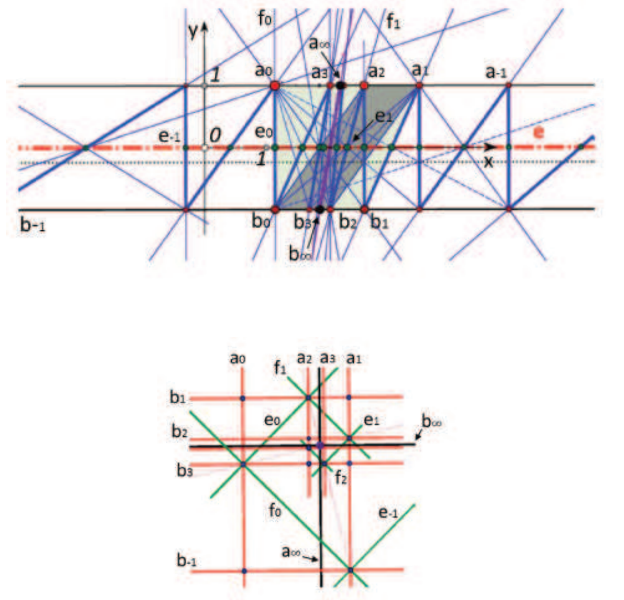

Figure 18: *Golden qh-polygon according to visualization method (α) by squares and rectangles (by dualizing the figure at top).*

In Figure 18 the points a, b represent the sides of the limit-quadrangle and their connection represents the pole of the spiral polygon (at right). Thereby the ratio of a with respect to a_1, a_0 reads as

$$
\begin{aligned}
r(a,a_1,a_0 =& r(a,a_3,a_2) = \ldots = 1:(3-\phi) \\
=& 1/5(2+\phi) = 0.723\ldots
\end{aligned} \tag{4}
$$

Visualization method (β) does not work here: In this model *qh*-circles occur as parabolas with common tangent e. It is impossible to construct non-trivial triples of mutually (outward) touching parabolas having a common tangent. Similarly, also method (γ) is not suited to *qh*-planes.

4.2 Projective cases

4.2.1 The hyperbolic plane (see 3.3)

Here we just refer to [4] and Figure 12 in 3.3.

4.2.2 The elliptic plane (*el*-plane)

Place of action is the full projective plane endowed with an elliptic absolute polarity. There are no similarities and no squares in the el-plane, such that visualisation method (α) cannot be performed. Because of the finite length of elliptic lines method (β) works well up to a certain number n of circles, see Figure 19. By choosing a suitably small unit for the scaling of the elliptic line this number can be any finite number n. For visualization purposes, this might be sufficient. If the *el*-circle radius would exceed the length l of a line one had to replace it by a circle with a radius modulo 1, what makes visualization very confusing. For e.g. a chain of golden *el*-circles on the sphere model of the *el*-plane it could be an idea to start with the largest possible *el*-circle, i.e. a great circle, and work from large to small, see Figure 20.

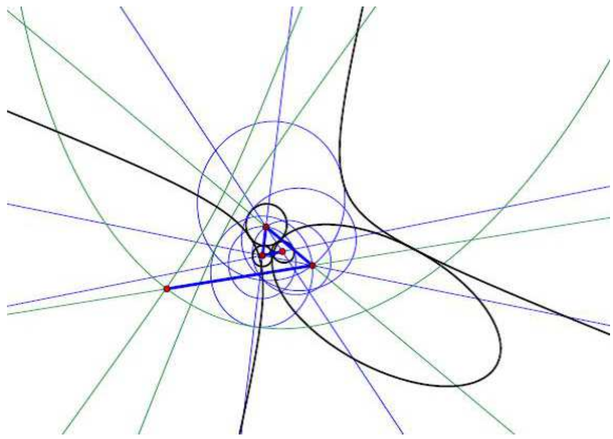

Figure 19: *Chain of Fibonacci circles in the projective model of the elliptic plane.*

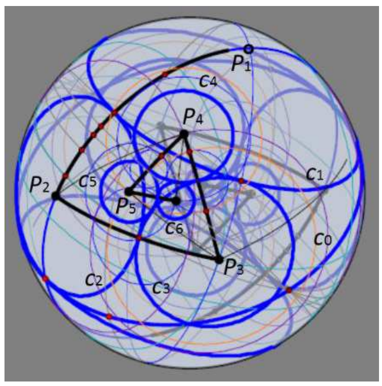

Figure 20: *Chain of Golden Circles on the Euclidean sphere representing the elliptic plane*

4.2.3 The dual Euclidean plane

is also called quasi-elliptic plane (*qe*-plane). Its absolute figure is a pair of conjugate imaginary lines i, j with a real intersection point U. A very convenient model of a qe-plane in the (projectively extendend) plane of visual perception (represented by a sheet of paper, the PC-screen or the blackboard) takes U as a proper point and i and j as the fixed lines of the (Euclidean) "right angle involution" in the pencil of lines with support U (see Figure 21 left). We use homogeneous Euclidean coordinates in both, the projectively enlarged Euclidean plane (e-plane) and the qe-plane. The transfer from the e-plane to the qe-plane can be carried out by the (regular) polarity $\Omega : \mathrm{P} \to \mathrm{L}$ defined by the regular imaginary conic section $x_0^2 + x_1^2 + x_2^2 = 0$ and the transformation matrix

$$T_\Omega = \begin{pmatrix} 1 & 0 & 0 \\ 0 & 1 & 0 \\ 0 & 0 & 1 \end{pmatrix}. \tag{5}$$

In the e-plane the parabolic distance measure in the point set P and the elliptic angle measure in the line set L are described by the usual Pythagoras formula (6) and Brauner's formula (7), see [2]:

$$d(P,Q) = \sqrt{(x_Q - x_P)^2 + (y_Q - y_P)^2} \tag{6}$$

with $x = \frac{x_1}{x_0}, y = \frac{x_2}{x_0}$ and

$$\tan\angle(p,q) = \sqrt{(-cr(p, p^\perp, q, q^\perp)}, \tag{7}$$

with $p^\perp$ e-orthogonal p, etc. These measures become a parabolic qe-angle measure in the line set L and an elliptic qe-distance measure in the point set P of a qe-plane. In our visualization of the qe-plane the qe-distance of two points P,Q which are non-collinear with U appears as the Euclidean angle between the lines UP, UQ, see Figure 21 (left). Thus the formulae (6), (7) just exchange their roles. Note that, similar to the isotropic case, qe-circles are not defined as (planar) point sets having constant distance from a centre point, but as conic sections touching the complex absolute lines i and j. This means that, in our visualization of a qe-plane, the absolute point U is a common (Euclidean) focus of the conic sections representing of qe-circles. One can choose one of the qe-circles as unit circle c and, similar to the isotropic case, extend the distance measure also to two parallel points $R, S(U)$, that are collinear with U : That additional distance can again be named *spacing* (*Sperrung*). It is defined by the difference of ratios as

$$d(R,S) := |r(S,E,U) - r(R,E,U)|, \tag{8}$$

with the point $E \in c$ acting as *unit point* on UR , see Figure 21 (right).

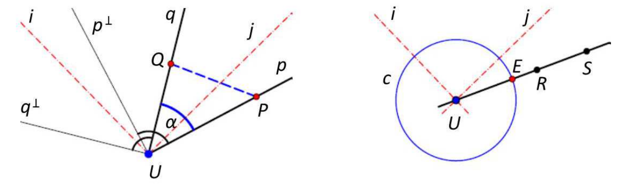

Figure 21: *qe-distance of non-parallel points (left) and of parallel points (right)*

(α) The dual of a Euclidean rectangle with sides a_1, b_1, a_2, b_2 is a quadrangle A_1, B_1, A_2, B_2 the diagonals e, f are orthogonal and intersect in U, (see Figure 22). For the dual of a Euclidean square the points $E := (A_1B_1) \cap (A_2B_2)$ and $F := (A_1B_2) \cap (A_2B_1)$ additionally are on orthogonal lines through U.

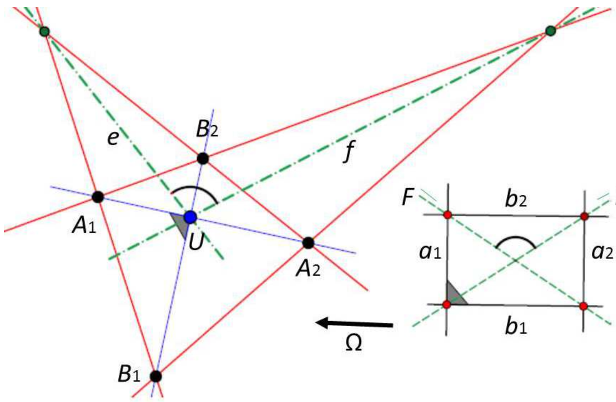

Figure 22: *qe-rectangles are quadrangles with orthogonal diagonals through U.*

So it is possible to transfer directly the Euclidean nested set of Golden Rectangles to the qe-plane, see Figure 23.

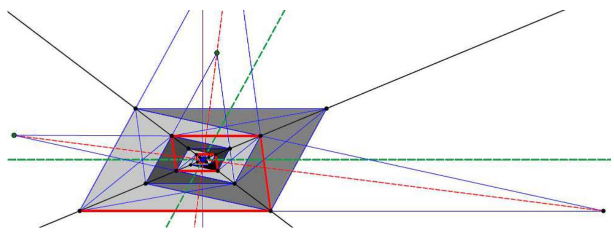

Figure 23: *Nested set of Golden qe-rectangles and a Golden qe-spiral polygon.*

(β) As a qe-circle is a conic section having U as one of its foci. Figure 24 shows that it is possible to construct a sequence of qe-circles, each touching the former two. Dealing with *radii*, however, would require a definition of qe-circles as a qe-distance set, which is not possible. This is why visualization method (β) does not work.

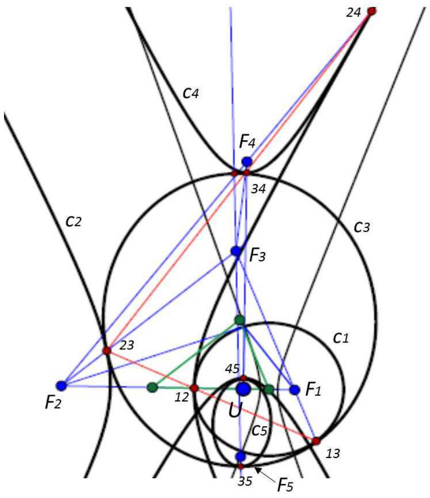

Figure 24: *A chain of qe-circles, one touching the two former qe-circles.*

(γ) To transfer the Euclidean Golden Root Spiral (Figure 8)) into the *qe*-plane model we have to construct a trilateral with angle ratio $\phi : \sqrt{\phi} : 1$. As Euclidean rotations with centre U are admitted, it becomes possible to also construct a *qe*-analog to the Golden Root Spiral, see Figure 25.

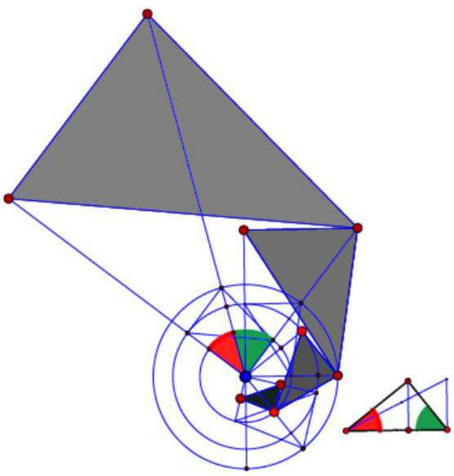

Figure 25: *A Golden quasi-elliptic root spiral.*

5 Conclusion and Outlook

The main subject of this paper is to show that visualizations of mathematical objects do not have to be performed in the classical Euclidean plane. Visualizations in other settings, like the Cayley-Klein planes or even spaces of higher dimensions, are justified as well. As an example we visualized the Golden Mean and the Fibonacci sequence in models of all possible Cayley-Klein planes. When doing so, visualisation methods based on typical Euclidean figures and properties have to be replaced by other methods. In this paper we propose three methods, which all work well in the Euclidean case. To transfer these methods in Cayley-Klein planes we use models conveniently adapted again to the plane of visual perception. Convenient means that constructions can be performed with available graphics software tools. In our paper we used Cinderella 2.8 for the figures. This CAD-software is distinguished by providing (planar) hyperbolic and elliptic geometry construction tools, too (see e.g. [15]). In some, but not all, Cayley-Klein planes we get visualizations of the Golden Mean and the Fibonacci sequence with modifications of the proposed Euclidean concepts.

Metallic Means generalize the Fibonacci sequence and the Golden Mean, see e.g. [13], [8]. The three presented methods could also be applied to visualize (generalized) Metallic Means. But as they all are defined as positive solutions of quadratic equations there will not occur essentially new results. Van der Laans and Rosenbuschs cubic generalizations of the Golden Mean have three-dimensional (Euclidean) visualizations by nested sets of boxes, thus generalizing the method (α) using squares and rectangles, see e.g. [5], [6] and [10]. Higher dimensional visualizations by nested sets of boxes are also known for Metallic Means, see [11]. For visualizations in non-Euclidean and Minkowski-spaces the method (β) (with hyper-spheres instead of circles, see [4]) seems to be natural and it is often the only possible method. Thereby one has to construct a chain of hyper-spheres, where the nth touches the former (n-1) hyper-spheres and their radii are proportional to Fibonacci numbers or elements of a geometric sequence. If we choose the radii according to a geometric sequence with proportionality factor ϕ or e.g. the Silver Mean one might call the occurring simplices of the centres of consecutive hyper-spheres Golden resp. Silver simplices.

References

[1] A. BEUTELSPACHER, B. PETRI, *Der goldende Schnitt*. Spektrum Akad. Verlag, B.I Mannheim 1996, ISBN 978-5860254042.

[2] H. BRAUNER, *Geometrie projektiver Räume*. Vol.II. B.I Mannheim 1976, ISBN 3-411-01513-6.

[3] O. GIERING, *Vorlesungen über höhere Geometrie*. Vieweg, Braunschweig 1982, ISBN 3-528-08492-8.

[4] S. MICK, G. WEISS, Fibonacci Triangles and Circle Chains and a Golden Bi-Arc Spiral in Non-Euclidean Planes. In H.-P. Schröcker and M. Husty, editors, *Proceedings of the 16th International Conference on Geometry and Graphics*, 415–422. Innsbruck University Press, 2014, ISBN 978-3-902936-46-2.

[5] R. PADOVAN, Dom Hans van der Laan and the Plastic Number. *Nexus IV, Architecture and Mathematics*, 181–193, 2002.

[6] L. ROSENBUSCH, *Räumliche Proportionen*. In O. Niewiadomski, editor, *Geometrie, Kunst und Wissenschaft 06*, Hauschild Verlag 2007, ISBN 978-38975-366-6.

[7] H. SACHS, *Ebene Isotrope Geometrie*. Vieweg, Braunschweig 1987, ISBN 978-3528084547.

[8] V. W. DE SPINADEL, The Family of Metallic Means, *Visual Mathematics* **1 (3)** (1999)

[9] H. WALSER, *The Golden Section* (transl. P. Hilton). The Mathem. Assoc. of America 2001, ISBN 0-8835-534-8.

[10] G. WEISS, V. W. DE SPINADEL, Remarks to classical cubic problems and the mean values of van der Laan and Rosenbusch, *Proooceedings of the 14th International Conference on Geometry and Graphics*, Article 235, 1–11, 2010.

[11] G. WEISS, From the Golden Rectangle to the Laan Box and more, *J. of Mathematics and Design*, **11** (2012), 14, ISBN 1515-7881.

[12] G. WEISS, V.W. DE SPINADEL, Bi-Arc Spirals an Minkowski Planes, In H.-P. Schröcker and M. Husty, editors, *Proceedings of the 16th International Conference on Geometry and Graphics*, 115–120. Innsbruck University Press, 2014, ISBN 978-3-902936-46-2.

[13] G. WEISS, V. W. DE SPINADEL, From George Odom to a new System of Metallic Means, *J. of Mathematics and Design* **12** (2013), 14, ISBN 1515-7881.

[14] `en.wikipedia.org/wiki/Golden-ratio`

[15] `http://www.heise.de/download/cinderella`

Gunter Weiss
e-mail: weissgunter@hotmail.com

University of Technology Vienna
Karlsplatz 13, 1040 Vienna, Austria

Sybille Mick
e-mail: mick@tugraz.at

University of Technology Graz
Kopernikusgasse 24, A-8010 Graz, Austria